

Membrane Surface Porosity and Pore Area Distribution Incorporating Digital Image Processing

^aMOHAMMAD ABBASGHOLIPOURGHADIM, ^{a*}MUSA BIN MAILAH, ^aINTAN ZAURAH, ^bA. F. ISMAIL, ^bM. REZAEI DASHTARZHANDI, ^cMEHDI ABBASGHOLIPOURGHADIM

Abstract-Hollow Fiber Membrane surface properties are crucial factors of evaluating the membrane performance in a special application. Hence, this study aims to develop an attractive and convenient digital image processing program package (IPP) for calculating membrane surface pore area, pore distribution and surface porosity. The results also can suggest how to control the spinning conditions towards fabricating a suitable membrane based on the requirements of a process. Different HFMs under various compositions and spinning conditions were fabricated and investigated in this study, including polyvinylidene fluoride (PVDF) with 12 – 22 wt.% and changes of dope extrusion flow rate and bore fluid flow rate. Fabricated HFMs were visualized and detected using Field Emission Scanning Electron Microscope (FESEM). The IPP changed the qualitative surface information from the outer surface FESEM images to quantitative results. The IPP determines the pore area, pore area distribution and surface porosity of membrane. The calculated surface porosity of the membranes was compared with the achieved value obtained from gas permeation test. There was no significant difference between the results of both methods confirming the applicability of IPP for the study of membrane surface properties. This work presents a novel approach in order to evaluate pore size, pore area and surface porosity of HFM material in different range.

Keywords-Hollow fiber membrane, Image processing, Pore area, Pore area distribution, Surface porosity

I. INTRODUCTION

Hollow fiber membranes have many application in large processes of industry such as gas separation, liquid separation and recently have become one of the most interest in water industry as well as wastewater treatment [1]. In addition, many researchers have investigated about the benefits of wastewater treatment and recycling. Wastewater treatment or reuse causes to decrease the wastewater discharge into environment [2]. Various studies have been done in the membrane separation technology, characterization of membrane structure including porosity, pore size and pore area distribution is one of the most important issue for membrane users and scientists as well as for membrane manufacturers[3]. The study of membrane morphology generally is related to the properties of membrane surface [4]. The porosity, pore

size and pore size distribution of the membranes can be obtained by several methods. They include molecular weight cut-off (MWCF) method [5], pressure of bubbles approach [6], field emission scanning electron microscopy (FESEM) [7], scattering the X-ray with small angle [8], atomic force microscopy (AFM) technique [[9],[10]], mercury intrusion method [11], liquid-liquid or liquid-gas displacement approach [12] and gas permeation test [13].

Image processing is a new and convenient method which is able to determine the membrane properties such as pore size, pore size distribution and porosity by digital analyzing. The dimension, shape and the number of pores in a special area of a membrane can be inspected by image processing analysis. Obtained images from the FESEM or SEM can be used for microscopy structure observation as well as digital image analyzing. As a result, the membrane morphology can be visualized such as effective surface porosity, pore size, pore shape and cross section studies [3]. In compared with FESEM, preparing the samples for SEM observation is easy, in which the fabricated membranes are dried and fractured in liquid nitrogen, then the fractured membranes are fixed perpendicularly to sample holder. Obtained images are analyzed by the digital images processing and analysis program NIH image [14].

In all kinds of membranes such as microfiltration or ultrafiltration, membrane porosity, pore size, pore size distribution and pore density are the important key factors for evaluation membrane performance and its separation [15].

Pereira studied the surface properties of the hollow fiber membranes by applying digital image processing [16]. The authors were then the results with the results obtained from scanning electron microscopy (SEM). First, the images were converted to grey scale and then to binary images by thresholding. The images were partitioned into black and white pixels. Eventually, the porosity of membrane was determined by image structure analyzer in three dimensions program [16]. However, they didn't classified the pore sizes on the surface of the membranes which decrease the accuracy of the obtained porosity. Based on the Shannon entropy maximum rule, the image's threshold segmentation means that after segmentation how much the information of statistical mean value of the image points ("1" or "0") include in a binary image [17]. In the reference [18] author used the

Locally Tuned Sine Nonlinear (LTSN) function to enhance the image intensity and contrast as well as colour restoration simultaneously.

Surface porosity, pore size and pore size distribution were determined in this paper by dealing with the FESEM photos of membranes using a digital image processing program package and then the results were further compared with the achieved results from gas permeation test.

II. EXPERIMENTATION

a. Membrane preparation

Commercial polyvinylidene fluoride (PVDF) polymer pellets were supplied by Arkema Inc., PA, USA. 1-Methyl-2-pyrrolidone (NMP) and Polyvinylpyrrolidone K90 (PVP) were used as solvent and non-solvent additives in the polymer solution dope.

The materials were dried in a vacuum oven for 48h at 80 ± 2 °C to remove the moisture. Hollow fiber Membranes were prepared by the combination of the wet-phase inversion method and the solution dispersion technique as described elsewhere [19]. PVP was first added to the solvent (NMP) under vigorous stirring. The PVDF polymer (12, 14, 16, 18, 20, 22 % wt) was then gradually added to the mixture with stirring simultaneously to have five different polymer solution. In order to have homogenous dope, polymer solution mixed at least 48 h under mechanical stirring at 55 °C and 575 Return Per Minute (RPM). The prepared solutions were degassed by ultra-sonication and loaded into a storage tank. The dopes were sent to the spinneret by pressurized Nitrogen (N₂). Distilled and tap water were used as bore fluid and external coagulant, respectively. Dope extrusion flow rate, bore fluid flow rate. Composition of solution were assumed as variables during the spinning process, other spinning parameters were kept constant. The nascent fibers were not drawn (no extension) as the take-up velocity of the hollow fiber was nearly the same as the falling velocity in the coagulation bath. A detailed description for hollow fiber spinning was given elsewhere ([20], [21]). The as-spun membranes were stored in water bath at room temperature for at least 72 h to remove the residual solvent and then stored in a 10 wt% Ethanol solution for at least 20 min. The membranes were then dried naturally in air at ambient condition before used for making test module.

Table 1 lists the specific details of spinning conditions.

Dope extrusion rate (mL/min)	2-4.7
Bore flow rate (mL/min)	0.7-1.6
Bore composition (wt.%)	Distilled water
External coagulant	Tap water
Air gap distance (cm)	0
Collection drum speed (m/min)	2.8
Spinneret OD/ID (mm)	1.1/0.55
Spinning dope temperature (°C)	ambient

External coagulant temperature (°C)	ambient
Bore fluid temperature(°C)	ambient

b. Gas permeation test, Pore size and porosity

The pore size and surface porosity to study mass transfer rate of porous asymmetric membranes in gas-liquid contacting processes are crucial of importance. The overall gas permeation through porous hollow fiber membranes is assumed to be a combination of Poiseuille (P_p) and Knudsen (P_k) flow regimes which by further assumption of straight and cylindrical pores, the total permeance is given by [22]:

$$J_{total} = \frac{F_{total}}{A\Delta p} = \varepsilon \frac{1}{lRT} \left[\frac{r^2}{8\eta} p + \frac{2r}{3} \left(\frac{8RT}{\pi M} \right)^{1/2} \right] \quad (1)$$

where J_{total} is total gas permeance ($\text{mol m}^{-2} \text{Pa}^{-1} \text{s}^{-1}$), R is universal gas constant ($8.314 \text{ J mol}^{-1} \text{ K}^{-1}$), T is absolute temperature (K), M is molecular weight of gas (kg mol^{-1}), r is mean pore radius (m), η is viscosity of gas (Pas), ε is surface porosity (A_p/A_T where A_p is area of pores and A_T is total area of membrane), l is effective pore length (m) and \bar{p} is mean pressure (Pa) ($p_u + p_d$)/2 where p_u is up stream pressure and p_d is downstream pressure. The permeance can be determined by measuring the gas permeation rate under a certain pressure difference across the membrane.

$$J_{total} = a\bar{p} + b \quad (2)$$

The values of a and b can be determined from the intercept and slope respectively in the J_{total} versus p plot [22]:

The mean modal pore radius is calculated by

$$r = \frac{16}{3} \left(\frac{a}{b} \right) \left(\frac{8RT}{\pi M} \right)^{1/2} \eta \quad (3)$$

The effective surface porosity over effective pore length ε/l can thus be calculated as follows:

$$\frac{\varepsilon}{l} = \frac{8\eta RT}{r^2} \quad (4)$$

Note that the effective pore length (l) is difficult to measure in practice and it is, in fact, not to necessary to measure it. Instead, it is convenient to use a combined parameter ε/l represent the porous structure of the membrane.

c. Field Emission Scanning Electron Microscopy (FESEM)

The membranes were put in holders and coated by sputtering platinum. A Zeiss Supra 35VP field emission scanning electron microscope (FESEM) with EDX analysis, from Carl Zeiss, Inc., (MN, USA) was used to observe the outer surface of the fabricated membranes.

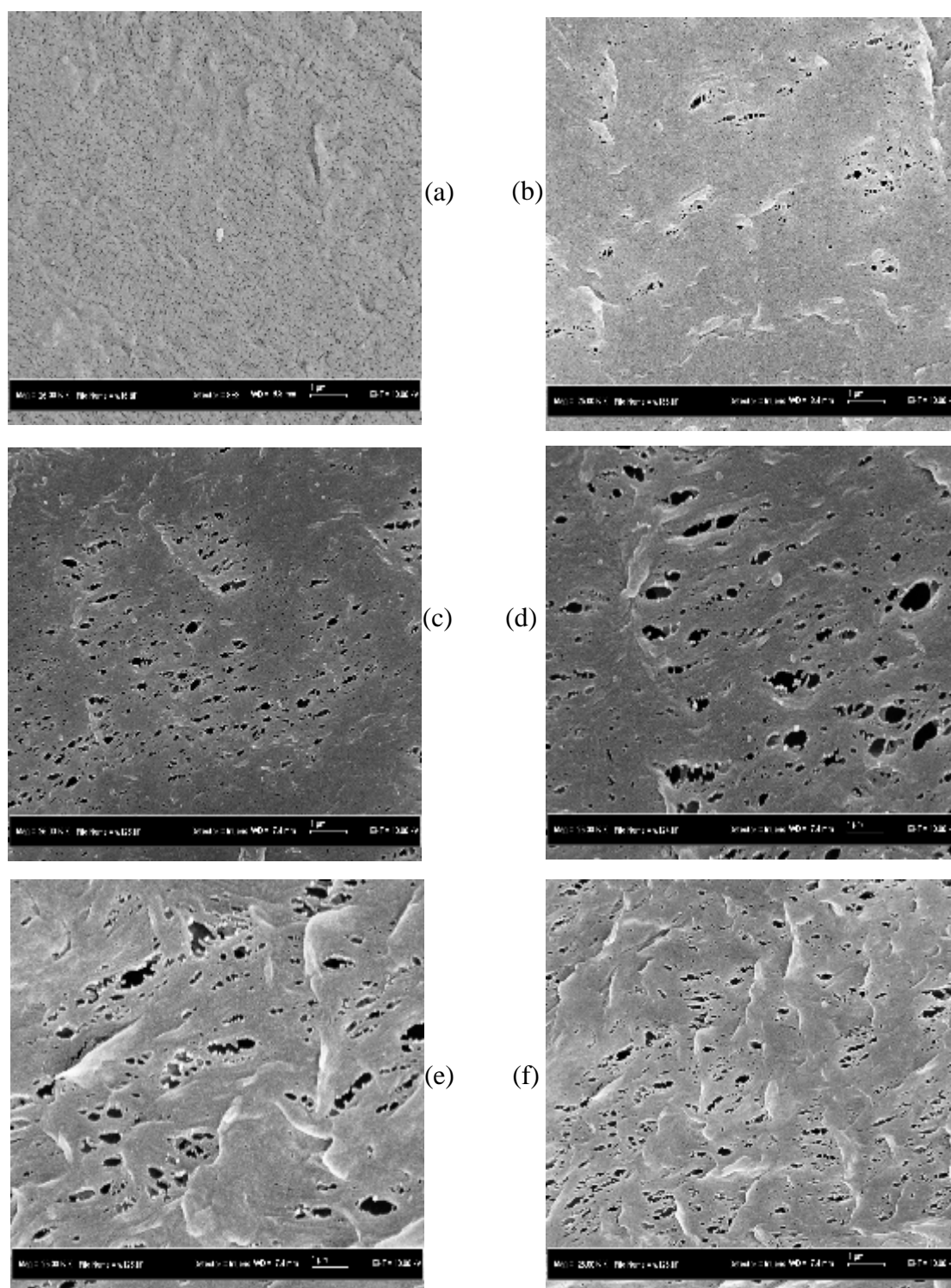


Fig. 1 FESEM surface images of hollow fiber membranes (a) PVDF 22% wt, PVP 3.06%, NMP 74.94%, (b) PVDF 20% wt, PVP 2.78%, NMP 77.22%, (c) PVDF 18% wt, PVP 2.5%, NMP 79.50%, (d) PVDF 16% wt, PVP 2.22%, NMP 81.78%, (e) PVDF 14% wt, PVP 1.94%, NMP 86.33%

d. Image analyses (Pre-processing)

For measuring the porosity, the pore size and the pore area distribution of the membrane, the obtained images

from FESEM with specific magnification were used. This image processing package separates each pore from its neighbours. Generally, the original images or grey

images from the outer surface of a porous membrane are binarized which are between zero and 255 pixels in which, pixels with low and high luminance were assumed as pore areas and background, respectively.

In the first step, the FESEM images were resized into 1000×1000 square pixels in order to transfer to the computer analysing. For filtration, a proper function was used to eliminate the noises from the colour images. Then an algorithm was used to increase the intensity of the images and edges. Before the classification, the images were adjusted as red green blue (RGB) images to detect of pore boundaries clearly.

The surface porosity of fabricated membranes were calculated by the following equation:

$$\varepsilon = \frac{\int_0^h (A_p) z dz}{(A_t)} \quad (5)$$

Where A_t is the total area of image, A_p is the area porosity at distance z , h is height of image.

In the binarized image each pore on the surface area of hollow fiber membrane is digitalized for measurement the pore size, porosity and pore area distribution. Pore distribution (pore's number / area) is defined by the

number of labeled pores on a chosen surface. To obtain accurate results, three modules for each membrane type were prepared. The results were averaged and mean surface porosity of three modules was assumed.

III. RESULTS AND DISCUSSION

The results obtained from the study is analyzed and discussed in the following subsections.

A. Field Emission Scanning Electron Microscopy (FESEM) and Image Analyses (Pre-processing)

Fig. 1 (a) shows FESEM surface micrograph of fabricated membrane. The FESEM images that qualitatively give the pore size, pore size distribution and the porosity of the membrane surface was attempted to be adjusted and give the best threshold. In fact, it is difficult to extract the exact pores with same threshold for various FESEM images of hollow fiber membranes. Hence, the triangle algorithm was extended to find on which side of the max peak the data goes the furthest and searches for the threshold within that largest range. The time of exposure, lightning and smooth or unsmooth outer surface of HFM are the significant criteria for adjusting the threshold. The FESEM micrograph after adjusting can be seen in Fig. 2(b).

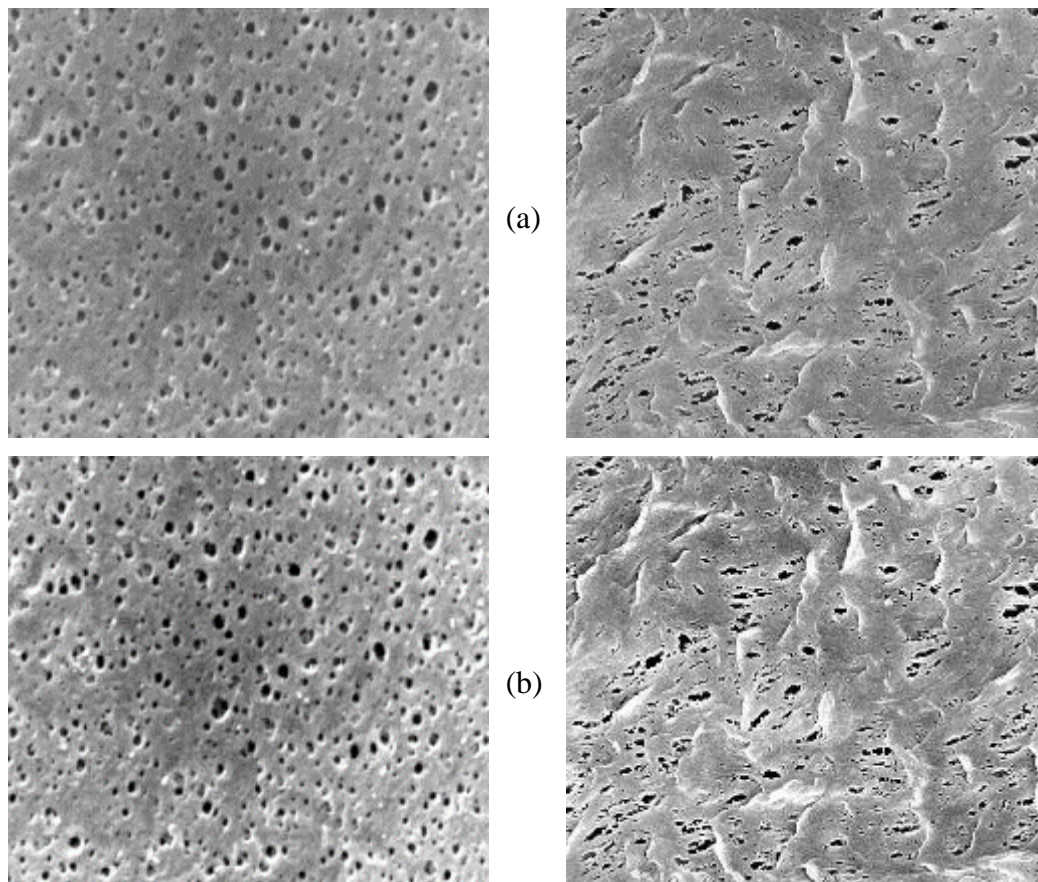
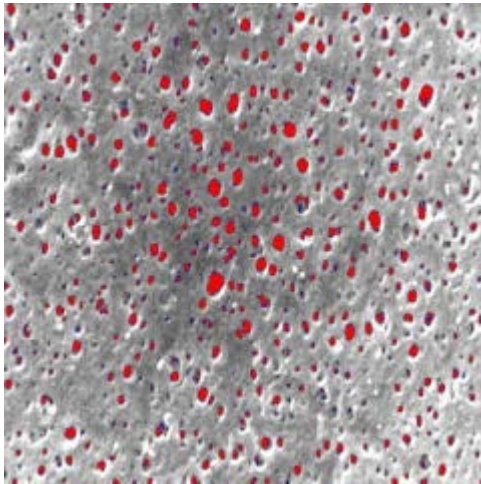


Fig. 2 FESEM outer images (a) original image; (b) adjusted image

It can be clearly observed that the boundary of pores are more visible in Fig. 2(b) in comparison with original FESEM image which make easier extraction of the pores for further analyzing in later sections.



As known, all the black colors in FESEM images cannot be assumed as real pores. Hence, the existence pores in images should be extracted and then classified. The classified pores of outer membrane surface by triangle algorithm is illustrated in Fig. 2.

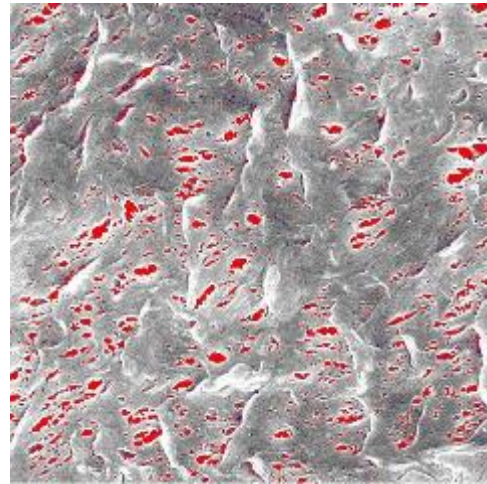


Fig. 3 pore extraction process of membrane outer surface by triangle algorithm

After pore classification, two groups of membrane pore could be easily detected from Fig. 3. First, the main and real pores that are separated with red color. Secondly, the blue color pores which assumed as failed pores.

Since solely the real pores are needed to determine the pore size, pore size distribution and surface porosity, the failed pores were ignored and the final extracted image was converted to binary images by data analyzing result which can be seen in Fig. 3.

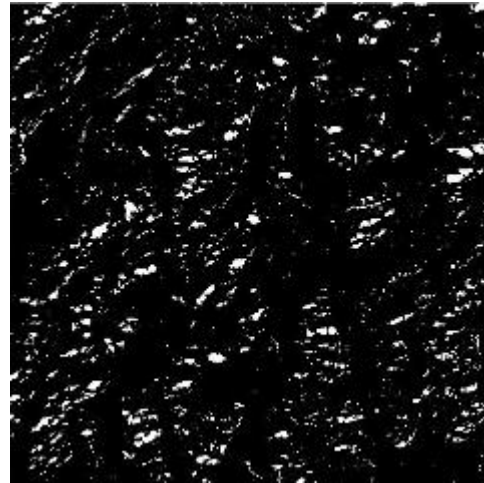
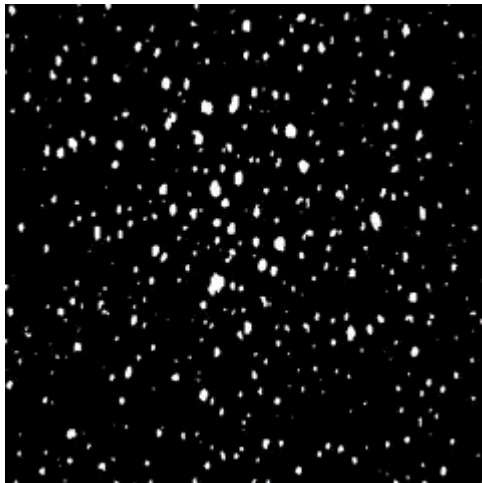


Fig. 4 real pore extracted by data analyzing result

The white color objects in Fig. 3 are final real pores extracted from Fig. 2(a) and the black part is the surface of the membrane with no pores.

Functions were used to determine pore size distribution and area based on the achieved binary image. The digital data after analyzing is shown in Fig. 5.

The area and distribution of the membrane surface pores will be calculated in the next section based on this figure.

B. Pore area distribution

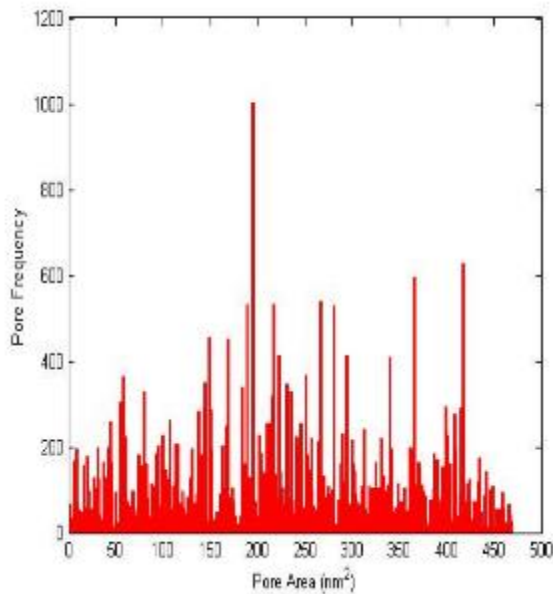


Fig. 4 real pore extracted by data analyzing result

The number of pores as well as their size can be extracted from the figure. This can help to modify the membrane surface towards a specific application.

C. Gas permeation

Since many parameters have effect on membrane structure during the fabrication, only 56 different samples were spun. Three modules for each type of membranes containing one hollow fiber with the effective length of 10 cm to obtain results that are more accurate were prepared. The hollow fibers were glued with epoxy glue at one end and the other end was potted to a stainless steel fitting. Purified nitrogen gas was supplied through the shell side of the modules and the N₂ pressure was increased at intervals of 0.5 bar. The permeation rates of gas coming out from the lumen side were measured by a soap-bubble flow meter. Each module was tested once and the average permeation rates were reported. Table 3 illustrates an example of gas permeation tests and shows how pore size and effective surface porosity are calculated.

Table 2 gas permeation timing for one sample (two modules) in which PVDF 18% wt, PVP 2.5%, NMP 79.50%, dope extrusion flow rate 5.00 cm³/min, bore fluid flow rate 1.7 cm³/min and speed of drum is 1.9 rpm.

P	t ₁₋₁	t ₂₋₁	t ₃₋₁	t ₁₋₂	t ₂₋₂	t ₃₋₂
0.5	13.5	13.3	13.34	14.82	14.64	14.24
1	7.3	7.44	7.62	7.8	8.18	8
1.5	4.94	5	4.98	5.38	5.44	5.26
2	3.44	3.3	3.26	3.64	3.44	3.62
2.5	2.56	2.68	2.6	2.68	2.8	2.82
3	2.44	2.06	2.2	2.36	2.26	2.28
3.5	1.88	1.8	1.76	1.8	1.94	1.9
4	1.5	1.56	1.54	1.62	1.5	1.74
4.5	1.28	1.29	1.31	1.4	1.5	1.32
5	1.19	1.09	1.16	1.19	1.22	1.18
5.5	0.94	0.93	0.95	1.15	1.09	1.14
6	0.87	0.84	0.86	1.03	0.91	1.07
6.5	0.84	0.82	0.71	0.87	0.78	0.84
7	0.75	0.65	0.63	0.78	0.75	0.79
7.5	0.59	0.58	0.6	0.62	0.59	0.69

Where, *p* is the pressure (bar) and *t* is the time (s) during gas permeation test. For each sample with two modules three times was repeated then the average time was used.

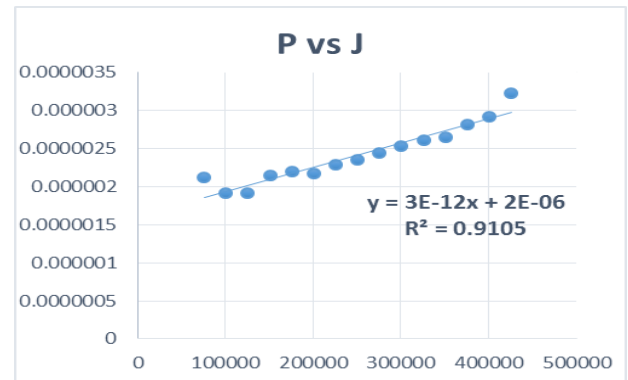


Fig. 6 mean pressure vs. gas permeation rate

As mentioned, pore size of hollow fiber membranes is calculated by Eq. 3 as follows:

$$r = \frac{16}{3} \left(\frac{a}{b}\right) \left(\frac{8RT}{\pi M}\right)^{\frac{1}{2}} \eta = 6.76E - 08$$

And, effective surface porosity per length based on Eq. 4 is defined as follows:

$$\frac{\varepsilon}{l} = \frac{8\eta RT}{r^2} = 231.6415$$

D. Surface porosity

The surface porosity of hollow fiber membranes was obtained by gas permeation test (GPT) and our image processing package (IPP) (see Table 3). From the table, it is revealed that the surface porosity decreases by increasing DER. This might be ascribed to the fact that the stress inside the spinneret increases by increasing the extrusion rate of solution.

In addition, it can be detected as well that the obtained results from both methods are not too dissimilar which can confirm the applicability of image processing method for porosity determination.

Table 3 surface porosity of different fabricated HFMs analysed by gas permeation instrument and our image processing package.

NO. HFM	DER	BF	CD	Porosity by GPT	Porosity by IPP
1	2	0.7	1.5	8.3	8.92
2	2.3	0.8	1.6	7.9	8.11
3	2.6	0.9	1.7	7.8	7.63
4	2.9	1	1.8	6.9	7.23
5	3.2	1.1	1.9	6.7	7.56
6	3.5	1.2	2	6.6	7.04
7	3.8	1.3	2.1	6.4	6.89
8	4.1	1.4	2.2	6	6.45
9	4.4	1.5	2.3	5.8	6.21
10	4.7	1.6	2.4	5.7	5.94

IV. CONCLUSIONS

In the present work, a system was designed to measure the membrane surface porosity, pore area distribution by detecting the changes of the pixel inside the FESEM images. PVDF hollow fiber membranes in different spinning conditions were spun and the real pores were extracted successfully from the original FESEM images of the hollow fiber membranes. Then the area and distribution of the pores were calculated based on the image processing package.

The surface properties were further determined by GPT and IPP methods. The results were near confirming the applicability of the method for calculating surface porosity.

ACKNOWLEDGEMENT

We would like to thank the Malaysian Ministry of Higher Education (MOHE) and UTM for providing the research funding and facilities. The research is executed using Vote No.: QJ130000.2513.02H15.

REFERENCES

- [1] K. Fukushi and L. Wang, "Study of ultrafiltration and nanofiltration for treating river water," in *Proceedings of the 49th National Waterworks Conference and Symposium, Japan*, 1998, pp. 188-189.
- [2] A. J. Hamilton, V. L. Versace, F. Stagnitti, P. Li, W. Yin, P. Maher, *et al.*, "Balancing environmental impacts and benefits of wastewater reuse," *WSEAS transactions on environment and development*, vol. 2, pp. 117-129, 2006.
- [3] C. Zhao, X. Zhou, and Y. Yue, "Determination of pore size and pore size distribution on the surface of hollow-fiber filtration membranes: a review of methods," *Desalination*, vol. 129, pp. 107-123, 2000.
- [4] M. Rezaei, A. Ismail, S. Hashemifard, G. Bakeri, and T. Matsuura, "Experimental study on the performance and long-term stability of PVDF/montmorillonite hollow fiber mixed matrix membranes for CO₂ separation process," *International Journal of Greenhouse Gas Control*, vol. 26, pp. 147-157, 2014.
- [5] I. Okazaki, H. Ohya, S. Semenova, S. Kikuchi, M. Aihara, and Y. Negishi, "Nanotechnological method to control the molecular weight cut-off and/or pore diameter of organic-inorganic composite membrane," *Journal of membrane science*, vol. 141, pp. 65-74, 1998.
- [6] F. Vigo, A. Bottino, S. Munari, and G. Capannelli, "Preparation of asymmetric PTFE membranes and their application in water purification by hyperfiltration," *Journal of Applied Polymer Science*, vol. 21, pp. 3269-3290, 1977.
- [7] L. Wang and X. Wang, "Study of membrane morphology by microscopic image analysis and membrane structure parameter model," *Journal of membrane science*, vol. 283, pp. 109-115, 2006.
- [8] B. Yang and A. Manthiram, "Comparison of the small angle X-ray scattering study of sulfonated poly (etheretherketone) and Nafion membranes for direct methanol fuel cells," *Journal of power sources*, vol. 153, pp. 29-35, 2006.
- [9] W. R. Bowen and T. A. Doneva, "Artefacts in AFM studies of membranes: correcting pore images using fast fourier transform filtering," *Journal of Membrane Science*, vol. 171, pp. 141-147, 2000.
- [10] D. F. Stamatialis, C. R. Dias, and M. N. de Pinho, "Atomic force microscopy of dense and asymmetric cellulose-based membranes," *Journal of membrane science*, vol. 160, pp. 235-242, 1999.
- [11] K. S. Sing and S. Gregg, "Adsorption, surface area and porosity," *Academic Press, London*, pp. 1-5, 1982.
- [12] K. S. McGuire, K. W. Lawson, and D. R. Lloyd, "Pore size distribution determination from liquid permeation through microporous membranes," *Journal of membrane science*, vol. 99, pp. 127-137, 1995.
- [13] M. Rezaei, A. F. Ismail, G. Bakeri, S. A. Hashemifard, and T. Matsuura, "Effect of general montmorillonite and Cloisite 15A on structural parameters and performance of mixed matrix membranes contactor for CO₂ absorption," *Chemical Engineering Journal*, vol. 260, pp. 875-885, 1/15/ 2015.
- [14] I. Masselin, L. Durand-Bourlier, J.-M. Laine, P.-Y. Sizaret, X. Chassera, and D. Lemordant, "Membrane characterization using microscopic image analysis," *Journal of Membrane science*, vol. 186, pp. 85-96, 2001.
- [15] T. Tweddle, C. Striez, C. Tam, and J. Hazlett, "Polysulfone membranes I. Performance comparison of commercially available ultrafiltration membranes," *Desalination*, vol. 86, pp. 27-41, 1992.
- [16] C. Pereira, R. Nobrega, and C. Borges, "Spinning process variables and polymer solution effects in the die-swell phenomenon during hollow fiber membranes formation," *Brazilian Journal of Chemical Engineering*, vol. 17, pp. 599-606, 2000.
- [17] L. Zhou, Y. Sun, and J. Zheng, "Automated color image edge detection using improved PCNN model," *WSEAS transactions on computers*, vol. 7, pp. 184-189, 2008.
- [18] S. Arigela and V. K. Asari, "A locally tuned nonlinear technique for color image enhancement," *WSEAS Transactions on Signal Processing*, vol. 4, pp. 514-519, 2008.
- [19] M. Rezaei, A. F. Ismail, S. A. Hashemifard, and T. Matsuura, "Preparation and characterization of PVDF-montmorillonite mixed matrix hollow fiber membrane for gas-liquid contacting process," *Chemical Engineering Research and Design*, vol. 92, pp. 2449-2460, 11// 2014.
- [20] A. M. Sakinah, A. F. Ismail, R. M. Illias, and O. Hassan, "Fouling characteristics and autopsy of a PES ultrafiltration membrane in cyclodextrins separation," *Desalination*, vol. 207, pp. 227-242, 2007.
- [21] J.-J. Qin, Y.-M. Cao, Y.-Q. Li, Y. Li, M.-H. Oo, and H. Lee, "Hollow fiber ultrafiltration membranes made from blends of PAN

- and PVP," *Separation and purification technology*, vol. 36, pp. 149-155, 2004.
- [22] D. Wang, K. Li, and W. Teo, "Porous PVDF asymmetric hollow fiber membranes prepared with the use of small molecular additives," *Journal of Membrane Science*, vol. 178, pp. 13-23, 2000.